Stratification and draught measurements of ceiling panels, underfloor cooling and fan-assisted radiators

Karl-Villem Võsa[a,b], *Egert* Eist[b], *Jarek* Kurnitski [a,b,c],

[a] FinEst Centre for Smart Cities (Finest Centre), Tallinn University of Technology, 19086 Tallinn, Estonia

[b] Nearly Zero Energy Buildings Research Group, Ehitajate tee 5, 19086 Tallinn, Tallinn University of Technology, Estonia

[c] Aalto University, School of Engineering, Rakentajanaukio 4 A, FI-02150 Espoo, Finland

Abstract. This paper reports the results of room conditioning unit measurements carried out in a NZEB test facility in 2021. Ceiling panels, fan-assisted radiators and existing underfloor heating contours were tested in several experimental configurations, operating with relatively high chilled water flow temperatures as these are all non-condensing systems. Time-controlled heating dummies were used to imitate internal heat gains along with the natural solar irradiation to vary the cooling demand. We quantify the vertical temperature gradients due to thermal stratification by measuring air temperatures at various heights. We also present the differences in thermal comfort of the tested systems, as we measure the air velocities and operative temperatures at points of occupancy with a standardised measurement probe. The gradient and operative temperature values affect the cooling emission efficiency which can be compared against an ideal cooling emitter. Measured results can be used to develop a new method for quantification of cooling emission efficiency. The annual emission efficiency can be assessed by applying measured values under different boundary conditions as inputs to simulation models.

Keywords. Cooling, thermal comfort, underfloor cooling, fan-assisted radiator, fan coil, ceiling panel, thermal stratification
DOI: https://doi.org/10.34641/clima.2022.170

1. Introduction

In the face of climate changes, current HVAC system design principles may not be sufficient for sustainable system operation in future climate conditions. Global policies target restricting the median warming to 1.5 °C by year 2100 [1]. Projections indicate more frequent, intense and longer-lasting heat waves [2], which has implications on the cooling loads and energy demands [3], as well as on the well-being of occupants [4], [5]. Therefore, it is of increasing importance to accurately assess emission efficiency of cooling systems.

According to EN 15316-2, space emission system efficiency is evaluated as a sum of different cooling set-point offsets, which reflect system inefficiencies in the distribution, control, and emission of the system [6]. This shifted set-point temperature is then used to calculate the annual cooling energy demand. A discrete set of values default values is given within the latest iteration of the standard, with the possibility of using product-specific values or different tabulated values from national annexes. However, procedures for measuring and calculating these parameter values are not specified in detail.

This study reports results from a set of experimental measurements that are going to be used in annual energy simulations, from which these set-point variations are going to be derived. In particular, thermal stratification, thermal comfort and system cooling capacities are analysed in detail.

2. Research methods

2.1 nZEB test facility

Tests of the cooling devices were conducted in the nZEB test facility at Tallinn University of Technology depicted in **Fig. 1**. Four different cooling devices were installed in the largest room of the facility – a 30 m^2 conference/classroom located on the east side of the building, seen in **Fig. 2**. This room has four windows, two on the east-facing external wall and one on both the north and south facades. The test room has a false ceiling and the whole building has a ventilated crawlspace.

Fig. 1 – Tallinn University of Technology nZEB test facility

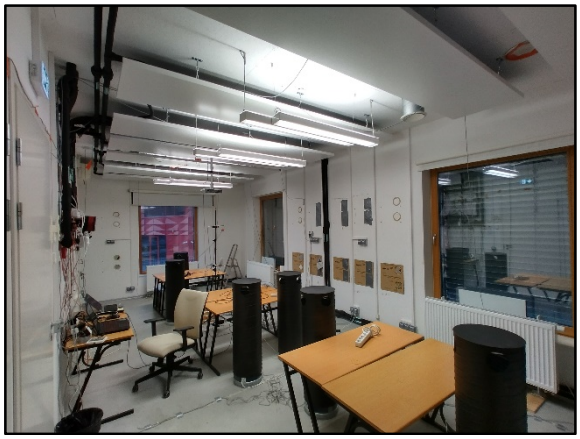

Fig. 2 – General view of the testing premises.

2.2 Ceiling panels

A total of eight ceiling panels (600 x 3000 mm) were installed using suspension cables at an installation height of 2.85 m, or 0.15 m from the ceiling (relative to the room facing side). The ceiling facing side was insulated with manufacturer provided mineral wool insulation plates. These ceiling panels were installed in four pairs, with the panels in series connection within the pair. Detailed geometry, positioning and hydraulic connections of the setup are shown in **Fig. 3.** Nominal conditions and cooling output for a serially connected pair is given in **Tab. 1**.

Tab. 1 - Ceiling panel specifications.

Parameter	Value
Supply temperature, °C	15.0
Return temperature, °C	19.0
Room air temperature, °C	25.0
Volume flow, l/h	76.3
Pressure loss, kPa	13.2
Cooling output per pair, W	354.7

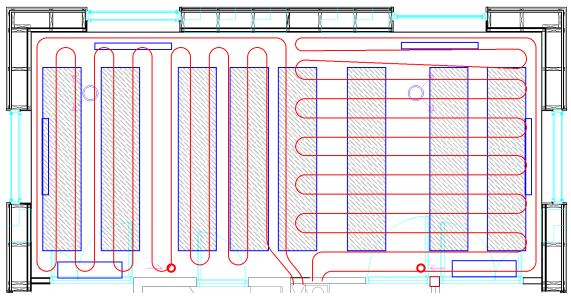

Fig. 3 – Positioning of ceiling panels and underfloor cooling loops.

Fig. 4 – Array of fans with the covering grille removed (left) and view of cooling radiator (right).

2.3 Fan-assisted radiator

Four type 22 steel panel radiators (600 x 1200 mm, two panels two convective fins) were installed in place of previously installed radiators under the windows of the test room. An array of fans is installed on top of the radiator under the cover grille to enhance the cooling output of the radiator. These fans displace air through the channel upwards into the room to prevent a cold down-draught to the floor. This fan speed is controlled according to the temperature difference between the air entering the channel and surface of the cooling panel. The specification and view of these radiators is shown in **Tab. 2** and **Fig. 4**.

Tab. 2 – Cooling radiator specifications.

Parameter	Value
Supply temperature, °C	15.0
Return temperature, °C	17.5
Room air temperature, °C	28.1
Volume flow, l/h	131.8
Cooling output, W	390.0

Tab. 3 – Fan coil unit specifications.

Parameter	Value
Supply temperature, °C	7
Return temperature, °C	12
Room air temperature, °C	27
Air volume flow, m³/h	390
Fan power input, W	28
Volume flow, l/h	511
Pressure loss, kPa	35.6
Cooling output, W	2120

2.4 Underfloor cooling

Existing underfloor heating loops were used for the testing of underfloor cooling. Supply and return lines before the manifold were retrofitted with 3-way and isolating valves to switch to the cooling circuit. Pe-PEX pipes (20 x 2.0 mm) are installed in a 40 mm screed layer with a 300 mm spacing between pipes. The cooling output of this set-up was estimated to be 750 W (25 W/m²) at operating conditions (14.0/17.0/26.0 °C supply/return/room air temperature). The geometry of the piping is shown in **Fig. 3**.

2.5 Fan coil unit

Two existing wall-mounted FCUs were used. Nominal cooling capacity and operating conditions at the lowest fan speed are listed in **Tab. 3**. The FCUs were operated at the lowest fan speed setting during the measurements.

2.6 Hydraulic installation and cooling generation

Chilled water was produced into a buffer tank with a heat pump. This heat pump operated on a single compressor speed; therefore, the chilled water set-point temperature was set to +10 °C with a hysteresis of ±2 °C to ensure there was sufficiently low temperature delivered to the mixing valve.

A 3-way mixing valve (3 mm travel) was used to control the supply temperature to the cooling devices. The valve was operated with a TA Slider 160 actuator, which got its input signal from a temperature control loop implemented in Python utilizing the simple-PID library. The following controller parameters were used: K_p=1800, K_i=60, K_d=13500, when considering the general PID formulation in equation (1).

$$u(t) = K_\mathrm{p} e(t) + K_\mathrm{i} \int_0^t e(\tau)\,\mathrm{d}\tau + K_\mathrm{d} \frac{\mathrm{d}e(t)}{\mathrm{d}t} \qquad (1)$$

Flow rate to the devices was set using a TA STAD-15 balancing valve. The flow measurement accuracy from the differential pressure over the balancing valve was however insufficient (4 % at best). Instead, a separate ultrasonic water meter was used to measure the volumetric flow rate in the secondary loop.

2.7 Measurement equipment

In the hydraulic part of the system, temperature sensors were installed in thermowells to monitor the chilled water supply and return temperatures both on the primary and secondary sides. Water flow rate was measured with an ultrasonic water meter installed on the return pipe of the secondary side.

A total of 25 sensors were used to measure various air and surface temperatures inside the tested room as well as air temperatures of the bounding rooms (corridor, toilet, two testing rooms) and behind the false ceiling and in the crawlspace. Sensor locations are shown in **Fig. 5** and **Fig. 6**.

A dedicated set of five thermo-anemometers, operative temperature sensor and a relative humidity sensor installed on a tripod were used to measure the gradients and air flow speeds at a pre-determined location for all systems.

FLIR E95 thermal camera was used to capture temperature distribution from the thermal images of the cooling devices. A fog generator was used to visualize the air distribution of the different systems. Ventilation air flow rates were set using both a capture hood and differential pressure manometer with valve position measurement.

Main specifications of the sensors used are listed in **Tab. 4**.

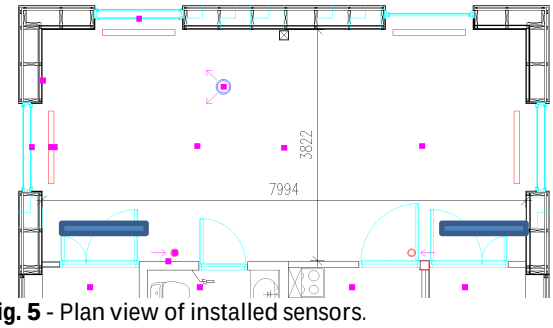

Fig. 5 - Plan view of installed sensors.

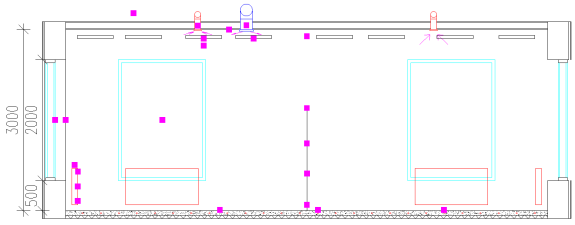

Fig. 6 - Section view of installed sensors.

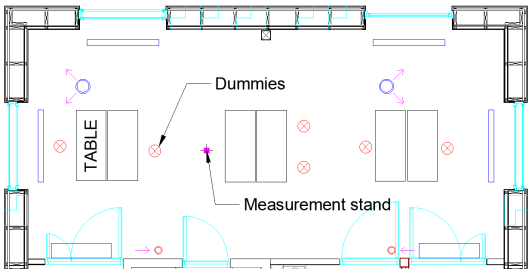

Fig. 7 - Room setup and positioning of heating dummies.

2.8 Internal heat gains

A total of six heating dummies were used in the tests, see the black cylinders in **Fig. 2**. These dummies have 3 incandescent lamps with a rated output of 3x60 W per dummy, in accordance with EN 14240 [7]. Two additional electric radiators with rated heat output of 1000 W were used to further provide a sufficient cooling load. Positioning of the dummies and radiators can be seen in **Fig. 7**.

2.9 Test conditions

The ceiling panels and radiators were tested at two nominal cooling outputs, HIGH output of 800 W (26.7 W/m²) and LOW output of 1200 W (40.0 W/m²), while the FCU was tested only at 1200 W and the underfloor cooling at 800 W. Targeted room air temperature during these tests was 25 °C. Supply and extract air flow rates were set to 1.5 l/(sm²), or 23 l/s per valve. Supplied air temperature was 19±1.5 °C.

Chilled water was supplied at temperatures between 15.0-18.5 °C, depending on the system in use. Volumetric flow rate to devices was kept at 300-350 l/h. External blinds were lowered for all tests to minimize variance from solar loads between the tests. Measurements took place in October-November.

Tab. 4 – Sensor specifications

Sensors	Meas. range	Accuracy
Fluid temperature	-50...+250 °C	±0.15+0.002|t| K
Air temperature	-40...+50 °C	±0.15 K
Surface temperature	-40...+50 °C	±0.15 K
Flow meter	0...3.125 m³/h	±3 %
Thermo-anemometer	0.05...5.00 m/s	±0.02 m/s
	-20...+80 °C	±0.20 K
Operative temp.	0...+45 °C	±0.20 K
Relative humidity	0...100 %	±1.50 %

2.10 Thermal comfort

Air stratification and vertical temperature distribution were assessed in two parts – the vertical air temperature difference γ_1 (head-ankle) according to standard EN16798-1 [8] and the total gradient between the ceiling and floor γ_{TOT}:

$$\gamma_1 = t_{1.1} - t_{0.1} \quad (2)$$

$$\gamma_{TOT} = t_{2.9} - t_{0.1} \quad (3)$$

where t_z is the air temperature at the specified height z in meters. The operative temperature probe was installed at a height of h = 1.10 m reclined to 30° from the vertical position. This value was compared to the air temperature at the same height, to assess whether a higher room air temperature can be allowed while keeping the same sensed temperature level of the occupant. Velocity data from the thermo-anemometers was also logged and analysed from the tripod setup. A typical set-up of this tripod is shown in **Fig. 8**.

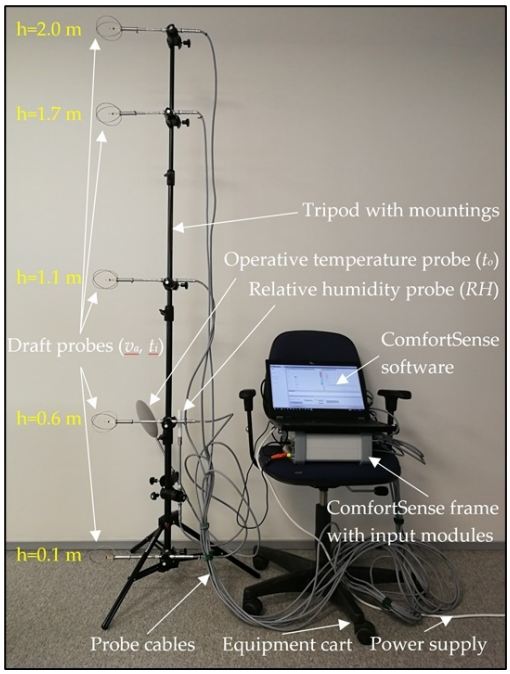

Fig. 8 – Thermal comfort measurement tripod.

3. Results

Hydraulic data and measured cooling outputs for each of the measurements is shown in **Tab. 5**.

3.1 Cooling power output

From **Tab. 5**, it is seen that the measured power is within ±10 % of the intended cooling outputs, except for the FCUs. Such deviations are inevitable, as the test room itself is part of the building susceptible to dynamic processes from both the external as well as internal boundaries (versus tailored test chambers, where all boundary conditions can be carefully measured and controlled).

Measurement accuracy of the cooling output is mostly affected by the low differential temperature in the supply and return temperatures of the chilled water. With temperature differences of 2...4 °C, the worst-case error from the temperature measurements can be 10...20% considering the around ±0.20 °C accuracy of the sensors at the measured temperatures. This could be improved with additional temperature differential sensors.

Tab. 5 – Test conditions, 1 h average.

System	Supply temperature, °C	Return temperature, °C	Room air temperature, °C	Chilled water flow rate, l/h	Cooling power, W	Cooling power, W/m²
Ceiling panels HIGH	15.09	17.96	25.38	335	1128	36.7
Ceiling panels LOW	18.50	20.60	26.66	337	820	26.7
Fan-assisted radiator HIGH	15.00	17.70	24.98	338	1061	34.6
Fan-assisted radiator LOW	15.25	17.41	25.14	345	869	28.3
Underfloor cooling	15.00	17.19	25.84	328	836	27.2
Fan coil units	17.00	21.00	25.88	334	1552	50.6

3.2 Temperature gradients

The underfloor cooling system had the highest temperature gradient by far, with γ_1 = 2.93 K/m and γ_{TOT} = 1.51 K/m (**Fig. 9**). This is the only measured system which at the measured cooling outputs falls into thermal comfort class II according to EN 16798-1 [8]. This falls in line with our expectations, as the cooled air mass near the floor is denser and does not induce a buoyancy effect to mix within the room. Conversely, the fan coil unit has almost no temperature gradient in the occupied zone, with only some temperature rise at h = 2.90 m, γ_1 = 0.14 K/m and γ_2 = 0.57 K/m, respectively ( ). High wall-mount is excellent for buoyancy-driven mixing within the room. The fans also help significantly to diminish the stratification.

Cooling panels and radiators both exhibited similar behaviour at the higher cooling output, with virtually no stratification in the occupied zone (**Fig. 11** and **Fig. 12**). At the lower cooling output, there is some stratification, γ_1 = 1.35 K/m and γ_2 = 0.55 K/m for ceiling panels and radiators, respectively.

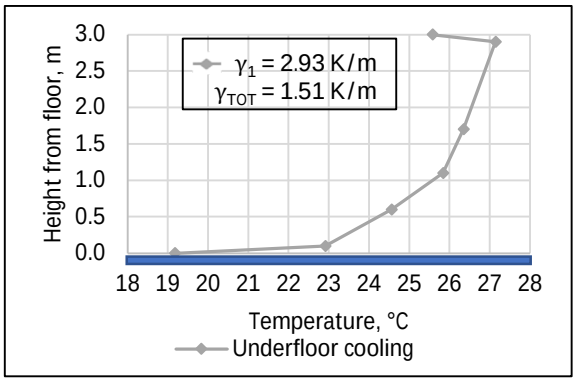

Fig. 9 - Measured gradient of underfloor cooling.

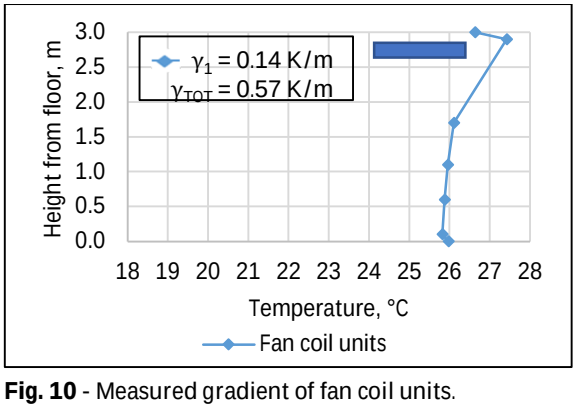

Fig. 10 - Measured gradient of fan coil units.

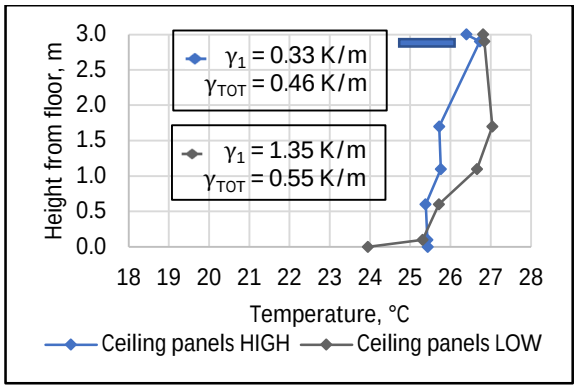

Fig. 11 - Measured gradient of ceiling panels.

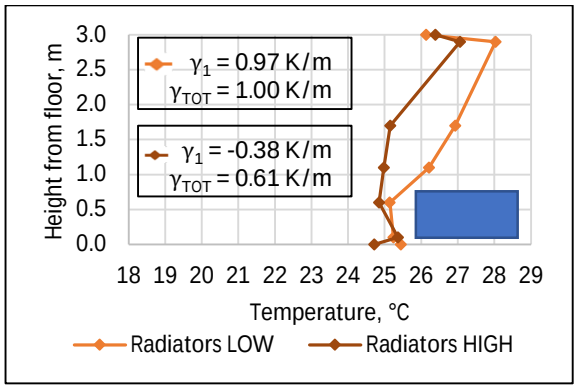

Fig. 12 - Measured gradient of radiators.

3.3 Operative temperature

We measured a sizable difference between the operative and air temperatures as shown in **Fig.** 13. Systems with greater surface areas (ceiling panels and underfloor cooling) have, with a difference as low as -1.28 °C for ceiling panels measured at the lower cooling output. Similarly, the FCUs have the opposite effect, with t_{op}-$t_{1.1}$ = 0.27 °C.

There is a causal effect between the measured gradient and t_{op}-$t_{1.1}$ value, which is why for both the ceiling panels and underfloor cooling, the lower cooling outputs have a higher temperature differential. Higher radiant heat exchange to the colder surface is offset by the lower temperature gradient value.

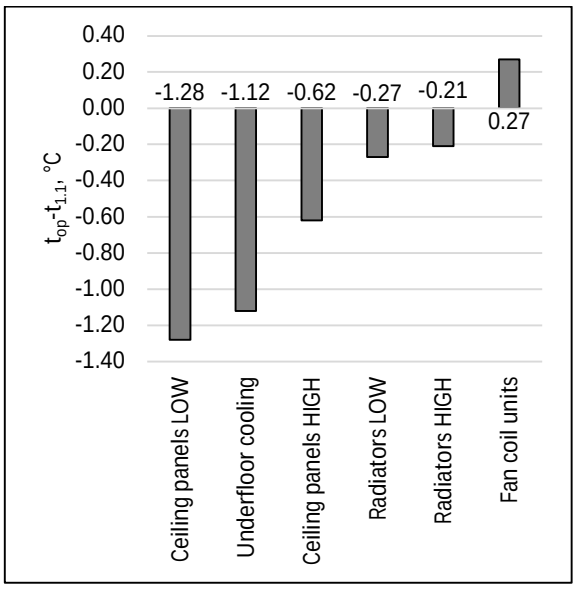

Fig. 13 – Measured operative and air temperature difference.

3.4 Air velocities

Air velocity measurements from the thermal comfort tripod are shown in **Tab 6**. These results are consistent with the thermal stratification seen in the previous section – higher velocities lead to higher mixing of air and vice versa.

For the FCU system, the air velocities in the occupied zone for both a seated and standing occupant are outside category III in accordance with EN 16798-1 [8]. Air velocities for the underfloor cooling are minimal, with average values of 0.02 m/s for both a seated and standing occupant.

We observed higher air velocities in the radiator HIGH tests compared to the radiator LOW tests, which was the excepted result as the fan speed was increased to the maximum output in those tests. Still, the measured air velocities were low enough to stay within the first category of thermal comfort.

Interestingly, this was not the case for ceiling panel HIGH and LOW outputs, with the air velocities being as high as 0.26 m/s at h = 1.70 m for the LOW case. These tests were conducted on different weeks, so it is possible that external factors skewed these measurement results. One would expect that if the higher cooling output achieved Cat. I in thermal comfort, the same would hold true for the lower cooling power.

3.5 Thermal imagery and measured surface temperatures

Thermal imagery of measured systems under selected test conditions are depicted in **Fig. 14**–**Fig. 17**. Visualized temperatures are based on a surface emission of ε=0.95.

The temperature distribution due to the fans drawing air through the radiator's panels can clearly be seen in . The perimeter of the radiator is cooler, as the convective heat transfer is lower due to lower air speeds.

Fig. 14 - Thermal image of radiator HIGH.

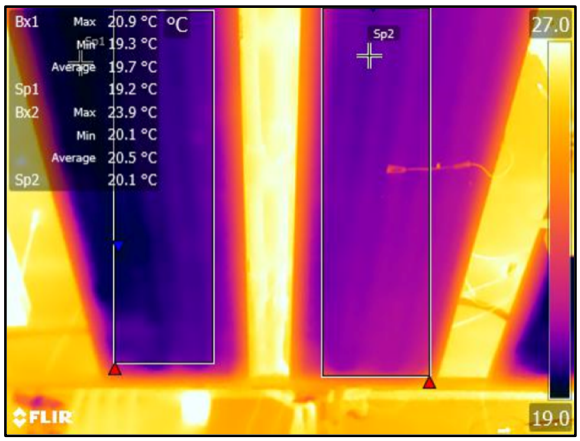

Fig. 15 - Thermal image of ceiling panels LOW.

Tab. 6 – Average air velocities measured on the tripod. Cat. I in green, Cat. II in yellow, Cat. III in orange and exceeding thermal comfort class boundaries in red, white for points outside occupied zone.

Height / System	Ceiling panels HIGH, m/s	Ceiling panels LOW, m/s	Radiators HIGH, m/s	Radiators LOW, m/s	Underfloor cooling, m/s	Fan coil units, m/s
2.90 m	0.19	0.06	0.11	0.19	0.08	0.19
1.70 m	0.07	0.26	0.08	0.07	0.02	0.88
1.10 m	0.04	0.13	0.12	0.04	0.02	0.45
0.60 m	0.10	0.03	0.09	0.10	0.02	0.25
0.10 m	0.03	0.03	0.06	0.03	0.02	0.61

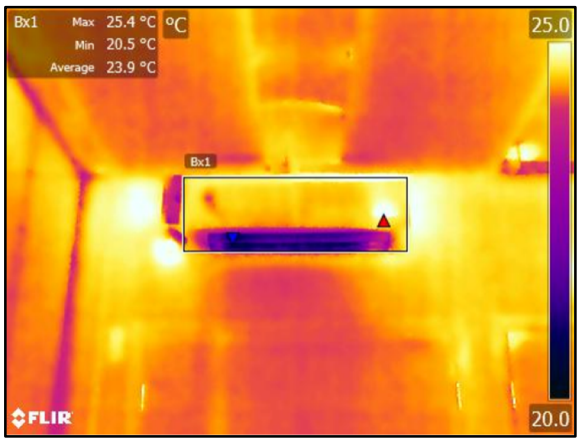

Fig. 16 - Thermal image of FCUs.

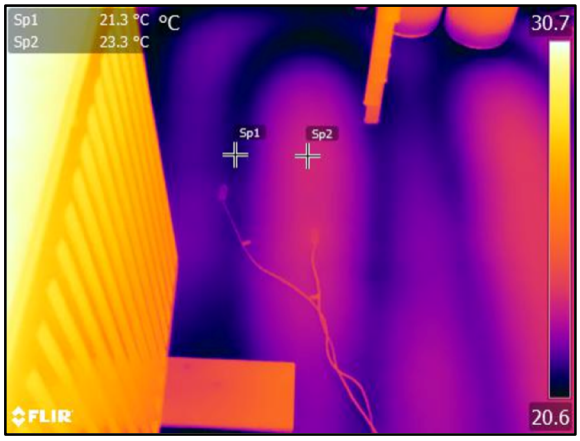

Fig. 17 - Thermal image of underfloor cooling.

Thermal image of a serially connected pair of cooling panels is shown in **Fig. 15**. The panel on the left has lower surface temperatures as it is connected directly to the supply line of the chilled water loop, while the supply of the panel on the right is connected to the return line of the panel on the left. In our measurements, there was an average of 1.0 °C surface temperature difference between the two panels.

The cooling coil of the FCU is seen in **Fig. 16**. This is mainly a convective system, the radiative heat transfer and its effect on operative temperature is minimal as the surface area and solid angle between the occupant and the coil is insignificant.

In **Fig. 17**, a section of the underfloor cooling system can be seen. A temperature difference of 2.0 °C was observed on top of the pipe and between the pipes (Sp1 and Sp2 on the image).

Surface temperatures were also measured at several locations, these results are tabulated in **Tab. 7**.

3.6 Limitations

Some limitations must be pointed out to understand which scope these results and conclusions should be interpreted.

Tab. 7 – Measured surface temperatures.

Device	Sensor	Temp., °C
Ceiling panels HIGH	1st in series	16.30
	2nd in series	17.75
Ceiling panels LOW	1st in series	19.36
	2nd in series	20.38
Radiators HIGH	h = 0.05 m	17.88
	h = 0.30 m	18.61
	h = 0.55 m	-
Radiators LOW	h = 0.05 m	17.37
	h = 0.30 m	19.02
	h = 0.55 m	19.41
Underfloor cooling	On supply pipe	17.85
	b/w supply pipes	19.03
	On return pipe	19.65
	b/w return pipes	20.37

These tests were conducted in autumn months of September-November, which are not in the typical cooling season for Estonia. This was an intentional choice to maintain boundary conditions to make the measurements results less susceptible to uncontrollable solar loads and external temperature swings. Furthermore, the internal heat gains used in the rooms were static loads, while cooling systems typically operate in dynamic conditions both from solar gains and from occupants, equipment, and lights. Thus, the inertia of the systems and control strategies are not assessed in this study.

There is also some effect on the internal surface temperatures and thus the operative temperatures from the chosen season of the tests. This is a function of the insulation of the external walls, which for our case is highly insulated with a thermal transmittance of 0.12 W/(m^{2}K). In poorly insulated boundaries, the mean radiant temperature of these boundaries can be significantly different depending on the outdoor temperature.

Risk of condensation was not assessed in detail. Latent load of the rooms was minimal, primarily from the supply air of the ventilation, which is typically more humid than during the tests. In real application, proper control measures must be taken to avoid condensation on the surfaces of the radiators, ceiling panels and the floor.

The tested systems have a relatively low cooling capacity by design (except the FCUs) and are suitable to be used in spaces where the cooling loads are <50 W/m^2. Furthermore, the measured gradients could vary throughout the room and may not describe the average gradient in the whole room. Therefore, the positioning of sensing equipment is crucial during the measurement and in the interpretation of the results. When considering the temperature gradients for the purposes of energy efficiency assessment, it must be noted that here only one or two cooling

output levels were measured. More measurements at different partial loads would give a more complete overview of the resulting temperature gradients, still subject to the effect of other boundary conditions as well, mainly the ventilation supply temperature and flow rate, but also the internal and external surface temperatures in the room.

4. Conclusions

Four room cooling devices were measured at a nominal cooling output 1200 W (40 W/m^2). This output was not reached for the underfloor cooling, where a capacity of 27 W/m^2 was reached instead at an average floor temperature of 19 °C. In rooms where the cooling loads are higher than 50 W/m^2, only the FCU has sufficient cooling capacity out of the tested devices. Other devices rest rely primarily on radiant heat transfer, which is limited in its cooling capacity.

Significant stratification was observed for the underfloor cooling. For a seated occupant, the head-ankle temperature difference of 2.93 K was measured, which barely achieves category II thermal comfort class for vertical temperature variation, while a standing occupant classifies to category III. Other systems exhibited milder stratification: overall temperature gradients were 1.00 K/m or less, with– all systems achieved thermal comfort category I.

In conjunction with the stratification, the difference between the operative and air temperature was assessed for all systems. In general, systems with larger radiant surfaces showed lower operative temperatures. This is an advantage for the energy efficiency of such radiant systems, as the same comfort level can be achieved at a higher air temperature. It is important to note that this temperature difference is influenced by the vertical temperature distribution as well, and from viewpoint of energy efficiency must be assessed simultaneously.

Finally, air velocities were also analysed. As expected, the fan coil units had the highest average velocities. Even at the lowest fan speed setting, a significant area around the FCU is far beyond the category III limit for air velocity, being unsuitable for typical office work. Other systems had lower velocities classifying to category I, except for the LOW ceiling panel, where likely the upward plume from the heating dummies prevailed instead.

5. Acknowledgement

This work has been supported by the Estonian Ministry of Education and Research, European Regional Fund (grant 2014-2020.4.01.20-0289), the Estonian Centre of Excellence in Zero Energy and Resource Efficient Smart Buildings and Districts, ZEBE (grant 2014- 2020.4.01.15-0016) funded by the European Regional Development Fund, by the European Commission through the H2020 project Finest Twins (grant No. 856602), the Estonian Research Council grant (PSG409) and the Association of the European Heating Industry EHI member companies Orkli, Purmo Group, Zehnder Group and Vasco.

6. References

[1] J. Rogelj *et al.*, 'Scenarios towards limiting global mean temperature increase below 1.5 °C', *Nature Climate Change*, vol. 8, no. 4, pp. 325–332, Apr. 2018, doi: 10.1038/s41558-018-0091-3.

[2] G. A. Meehl and C. Tebaldi, 'More Intense, More Frequent, and Longer Lasting Heat Waves in the 21st Century', *Science*, vol. 305, no. 5686, pp. 994–997, 2004, doi: 10.1126/science.1098704.

[3] D. D'Agostino, D. Parker, I. Epifani, D. Crawley, and L. Lawrie, 'How will future climate impact the design and performance of nearly zero energy buildings (NZEBs)?', *Energy*, p. 122479, 2021, doi: https://doi.org/10.1016/j.energy.2021.122479.

[4] D. M. Hondula, R. C. Balling, J. K. Vanos, and M. Georgescu, 'Rising Temperatures, Human Health, and the Role of Adaptation', *Current Climate Change Reports*, vol. 1, no. 3, pp. 144–154, Sep. 2015, doi: 10.1007/s40641-015-0016-4.

[5] D. Bienvenido-Huertas, C. Rubio-Bellido, D. Marín-García, and J. Canivell, 'Influence of the Representative Concentration Pathways (RCP) scenarios on the bioclimatic design strategies of the built environment', *Sustainable Cities and Society*, vol. 72, p. 103042, 2021, doi: https://doi.org/10.1016/j.scs.2021.103042.

[6] C. E. de Normalisation, 'European Standard EN 15316-2: 2017. Energy performance of buildings. Method for calculation of system energy requirements and system efficiencies. Space emission systems (heating and cooling), Module M3-5', M4-5., Tech. rep., CEN, Bruxelles, BE, 2017.

[7] B. CEN, '14240: 2004 Ventilation for buildings–Chilled ceilings–Testing and rating offers a testing method for chilled ceilings'. CEN, 2004.

[8] EN 16798-1: 2019, 'Energy Performance of Buildings—Ventilation for Buildings—Part 1: Indoor Environmental Input Parameters for Design and Assessment of Energy Performance of Buildings Addressing Indoor Air Quality, Thermal Environment, Lighting and Acoustics—Module M1-6'. European Committee for Standardization Brussels, Belgium, 2019.